Molecular Therapy
Methods & Clinical Development
Original Article

Empowering Retinal Gene Therapy with a Specific Promoter for Human Rod and Cone ON-Bipolar Cells

Elmar Carlos Hulliger,[1] Simon Manuel Hostettler,[1] and Sonja Kleinlogel[1]

[1]Institute of Physiology, University of Bern, 3012 Bern, Switzerland

Optogenetic gene therapy holds promise to restore high-quality vision in blind patients and recently reached clinical trials. Although the ON-bipolar cells, the first retinal interneurons, make the most attractive targets for optogenetic vision restoration, they have remained inaccessible to human gene therapy due to the lack of a robust cell-specific promoter. We describe the design and functional evaluation of 770En_454P(h*GRM6*), a human *GRM6* gene-derived, short promoter that drives strong and highly specific expression in both the rod- and cone-type ON-bipolar cells of the human retina. Expression also in cone-type ON-bipolar cells is of importance, since the cone-dominated macula mediates high-acuity vision and is the primary target of gene therapies. 770En_454P(h*GRM6*)-driven middle-wave opsin expression in ON-bipolar cells achieved lasting restoration of high visual acuity in the *rd1* mouse model of late retinal degeneration. The new promoter enables precise manipulation of the inner retinal network and paves the way for clinical application of gene therapies for high-resolution optogenetic vision restoration, raising hopes of significantly improving the life quality of people suffering from blindness.

INTRODUCTION

Optogenetic and gene supplementation therapies to restore vision are already performed on human patients[1] (Table 1). In the sophisticated neuronal network of the retina,[2] targeting therapeutic genes to specific cell types to achieve precise intervention is often imperative. While the photoreceptor cells and the retinal pigment epithelium are targets for gene therapy at early stages of retinal degeneration, the bipolar cells make promising targets for gene therapy at late stages of retinal degeneration, when most photoreceptors are lost. The bipolar cells are the first interneurons of the retina that receive direct input from the photoreceptors. They are divided into ON- and OFF-type bipolar cells that respond to either light increments or light decrements, respectively, forming the foundation for contrast vision.[3] It was previously shown that optogenetic sensitization of ON-bipolar cells (OBCs) to light in a photoreceptor-less, blind murine retina can restore light responsiveness and complex inner retinal signaling, resulting in diverse receptive-field types in the retinal ganglion cell population.[4,5] Channelrhodopsin-2,[5] rhodopsin,[6] and chimeric Opto-mGluR6[4] have all been expressed in the OBCs of blind *rd1* mice to restore functional vision at the retinal, cortical, and behavioral levels. Photoswitchable chemical ligands attached to cysteine-mutated modified glutamate receptors (LiGluRs) equally restored visual responses in *rd1* mice when targeted to the OBCs.[7] Besides optogenetic approaches, OBCs also present attractive targets for gene supplementation therapies treating congenital stationary night blindness (CSNB). Most mutations causing CSNB are found in OBC-specific genes that encode proteins of the mGluR6 signalosome, such as *NYX, GRM6, GPR179*, *LRIT3*, *GNB3*, and *TRPM1*.[8]

Although OBCs were successfully targeted in the mouse retina, they remained inaccessible to gene therapy in the human retina due to the lack of molecular tools; in particular, a specific promoter that can drive strong transgene expression in human OBCs. A reason for the divergence of promoter performance in murine and human retinas is the prominent inter-species functional variability of molecular tools.[9] Further, OBCs are located deep within the retinal tissue, making them less accessible to viruses. They also appear rather non-permissive to viral transduction and require highly specialized promoters.[9] This becomes evident by the fact that specific targeting of diverse retinal cell types, but excluding OBCs, was recently achieved in the primate and human retina using a combinatorial screen of synthetic promoters and novel adeno-associated virus (AAV) capsid variants. OBC-specific expression is important not only for restoring precise retinal signaling with an optogenetic gene therapy but also for reducing the risk of toxic and/or inflammatory reactions previously linked to unspecific protein expression using ubiquitous promoters.[10] Due to the species specificity of molecular tools, promoter function must inevitably be tested in human tissue. A valuable pre-clinical model to test promoter specificity and efficacy in human tissue is the post-mortem human retinal explant (HRE). Since promoter specificity is independent of the viral administration route, a whole-eye *in vivo* gene therapy is not required.

The 9.5-kb full-length murine *Grm6* promoter is known to exclusively drive expression in OBCs[11] and was successfully used in a transgenic

Received 25 February 2020; accepted 9 March 2020;
https://doi.org/10.1016/j.omtm.2020.03.003.

Correspondence: Sonia Kleinlogel, Institute of Physiology, University of Bern, 3012 Bern, Switzerland.
E-mail: sonja.kleinlogel@pyl.unibe.ch

source: https://doi.org/10.7892/boris.144033 | downloaded: 24.5.2020

This is an open access article under the CC BY-NC-ND license (http://creativecommons.org/licenses/by-nc-nd/4.0/).

Table 1. Ongoing AAV Gene Replacement and Gene Supplementation Trials in the Retina

ClinicalTrials.gov identifier	Disease	Gene	Target cells	Vector	Delivery	Phase	Drug	Start	Estimated Date of completion
NCT03328130	Autosomal recessive RP	*PDE6B*	PRs	AAV2/5	SR	I/II	HORA-PDE6B	2017	2022
NCT03374657	Autosomal recessive RP	*RLBP1*	RPEs	AAV2/8	SR	I/II	CPK850	2018	2025
NCT03252847	X-linked RP	*RPGR*	PRs	AAV2	SR	I/II		2017	2020
NCT03116113	X-linked RP	*RPGR*	PRs	AAV2/8	SR	II/III		2017	2020
NCT03316560	X-linked RP	*RPGR*	PRs	AAV2	SR	II/III	AGTC-501	2018	2024
NCT01482195	RP	*MERTK*	RPEs	AAV2	SR	I		2011	2023
NCT02556736	Advanced RP	ChR2	RGCs	AAV2	IVT	I/IIa	RST-001	2015	2033
NCT03326336	Non-syndromic RP	ChrimsonR	RGCs	AAV2(7m8)	IVT	I/IIa	GS030	2018	2024
NCT03507686	Choroideremia	*REP1*	RPE	AAV2	SR	II		2017	2020
NCT03496012	Choroideremia	*REP1*	RPE	AAV2	SR	III		2017	2020
NCT02407678	Choroideremia	*REP1*	RPE	AAV2	SR	II		2016	2021
NCT02341807	Choroideremia	*REP1*	RPE	AAV2	SR	I/II		2015	2019
NCT03001310	Achromatopsia	*CNGB3*	PRs	AAV2/8	SR	I/II		2016	2019
NCT03278873	Achromatopsia	*CNGB3*	PRs	AAV	SR	I/II		2017	2023
NCT02599922	Achromatopsia	*CNGB3*	PRs	AAV2	SR	I/II		2016	2022
NCT02935517	Achromatopsia	*CNGA3*	PRs	AAV2	SR	I/II	AGTC-402	2017	2021
NCT02610582	Achromatopsia	*CNGA3*	PRs	AAV2/8	SR	I/II		2017	2021
NCT00516477	Leber congential amaurosis	*RPE65*	RPEs	AAV2	SR	I/II	VN	2007	2024
NCT01208389	Leber congential amaurosis	*RPE65*	RPEs	AAV2	SR	I/II	VN	2010	2026
NCT00999609	Leber congential amaurosis	*RPE65*	RPEs	AAV2	SR	III	VN	2012	2029
NCT02946879	Leber congential amaurosis	*RPE65*	RPEs	AAV2/5	SR	I/II	AAV OPTIRPE65	2016	2023
NCT00481546	Leber congential amaurosis	*RPE65*	RPEs	AAV2	SR	I		2007	2026
NCT03597399	Leber congential amaurosis	*RPE65*	RPEs	AAV2	SR	post-authorization	VN	2019	2029
NCT02416622	X-linked retinoschisis	*RS1*	PRs, BCs	AAV2	IVT	I/II		2015	2022
NCT02317887	X-linked retinoschisis	*RS1*	PRs, BCs	AAV2/8	IVT	I/II	RS1 AAV Vector	2014	2021
NCT02065011	Usher syndrome 1B	*MY07A*	PRs	LV	SR	I/II	UshStat	2013	2035
NCT01505062	Usher syndrome 1B, RP	*MY07A*	PRs	LV	SR	I/II	SAR421869	2012	2020
NCT01367444	Stargardt disease	*ABCA4*	PRs	LV	SR	I/II	SAR422459	2011	2019
NCT01736592	Stargardt disease	*ABCA4*	PRs	LV	SR	I/II	SAR422459	2012	2034

RP, retinitis pigmentosa; AAV, adeno-associated virus; LV, lentivirus; PRs, photoreceptor cells; RGCs, retinal ganglion cells; SR, subretinal injection; RPEs, retinal pigment epithelial cells; IVT, intravitreal injection; VN, voretigene neparvovecrzyl; BCs, bipolar cells.

mouse line to drive expression in all OBCs of the murine retina.[4] For AAV-based gene therapies, however, short promoter sequences are required, since the packaging capacity of an AAV is limited (approximately 4.7 kb) and does not accommodate endogenous promoters of several kilobases in length. In this respect, enhancer promoter combinations derived from *Grm6* have proven most successful in driving transgene expression in murine OBCs. A short 200-bp *Grm6* enhancer in combination with a basal viral simian virus 40 (SV40) promoter (200En-SV40)[12] was first used for ectopic channelrhodopsin-2 expression in OBCs.[5] Introducing a quadruple repetition of the 200-bp *Grm6* enhancer preceding the SV40 basal promoter (4xGRM6-SV40) was later shown to increase transgene expression in the murine retina.[13] Unfortunately, 4xGRM6-SV40 was unable to drive transgene expression in OBCs of the degenerated *rd1* mouse retina and led to significant off-target expression in *ex vivo* cultures of human post-mortem retinas.[14] More recently, an entirely murine *Grm6*-based short promoter was designed (200En-mGluR500P) that drives gene expression in the wild-type C57BL/6 mouse retina

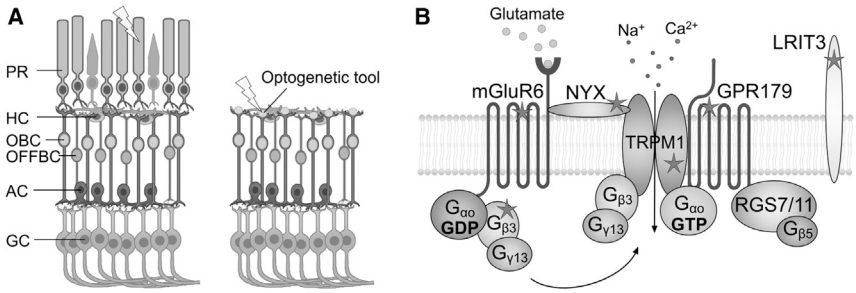

Figure 1. ON-Bipolar Cells as Therapeutic Targets in Retinal Degeneration

(A) Schematic of a healthy retina on the left and a degenerated retina lacking photoreceptors on the right. PR, photoreceptor; HC, horizontal cell; OBC, ON-bipolar cell; OFFBC, OFF-bipolar cell; AC, amacrine cell; GC, ganglion cell. In retinal degeneration, the most distally remaining cells of the visual pathway are the OBCs, which can be engineered into "replacement photoreceptors" by an optogenetic gene therapy. (B) The mGluR6 signalosome in the dendritic tips of OBCs and proteins therein that are affected by loss-of-function mutations—indicated with stars—in congenital stationary night blindness. OBC-targeted gene supplementation therapies can restore function. mGluR6 is a metabotropic glutamate receptor that activates trimeric Gao/Gb3/Gy13 gating the cation channel TRPM1. LRIT3 is required for proper localization of TRPM1, and GPR179 and NYX are scaffolding proteins.

with high OBC specificity.[15] However, expression in OBCs of the degenerated retina and in human tissue was not investigated, and transgene expression in the murine retina was almost exclusively restricted to the rod-type OBCs (rOBCs). Since high-resolution macular vision is mediated by cones and cone-type OBCs (cOBCs) of the midget pathway in a human, it is imperative for a gene therapy targeting the OBC population to achieve robust expression in the cOBCs.

Here, we introduce a novel synthetic promoter derived from the human *GRM6* gene, consisting of a core promoter element and an enhancer element, which drives transgene expression in OBCs in a robust and highly specific (approximately 90%) manner when delivered by an AAV gene therapy, not only in late degenerated murine retinas but particularly also in human *ex vivo* retinas. Proof of functionality in the human retina is important due to the known variability of cell-type targeting by synthetic promoters across species.[9] A further advantage of the novel 770En_454P(h*GRM6*) promoter is its ability to drive strong expression in cOBCs of the human macula, with no selectivity for rOBCs over cOBCs; this is not only important because the cone-dominated fovea mediates high-acuity vision, but also because current retinal gene therapies (Table 1) almost exclusively target the macular region, which is most permissive to AAV transduction in humans and primates.[16] Further advantages of the 770En_454P(h*GRM6*) promoter are that it mediates low off-target gene expression in other retinal cell types of the human retina and that it complies in size (1.2 kb) with other promoters used in AAV gene therapies.

The 770En_454P(h*GRM6*) promoter paves the way toward OBC-targeted gene therapies, including high-resolution optogenetic vision restoration and treatment of CSNB, thereby bringing hope to millions of people suffering from photoreceptor degeneration. Giving access to OBCs for genetic manipulations makes 770En_454P(h*GRM6*) also a welcome tool to unravel inner retinal signaling across species, across health and disease, and across different approaches of prosthetic restoration.

RESULTS

The OBCs make promising targets for gene therapy, either to replace malfunctioning genes causative of congenital stationary night blindness or to restore vision by an optogenetic supplementation therapy when photoreceptors are lost (Figure 1). Bipolar cells are the first interneurons of the retinal neuronal network and remain relatively well preserved in advanced retinal degeneration,[17] which allows optogenetic restoration of sophisticated visual signaling[4,6] (Figure 1A). Preclinical endeavors are underway that supply functional versions of mutated genes to the OBCs to restore the mGluR6 signaling pathway in CSNB patients[8] (Figure 1B) and, with that, OBC function and vision.[18] The mGluR6 receptor is exclusively expressed in the OBCs;[4,11] therefore, the *Grm6* gene makes a valuable target for promoter design. It was shown that the murine *Grm6* enhancer in combination with the SV40 viral promoter is able to drive OBC-enriched expression of exogenous transgenes in the murine retina.[13]

Changes in *Grm6* Transcription during Retinal Degeneration

Since we recently showed that expression from the 4xGRM6-SV40 promoter is severely downregulated in 8-week-old *rd1* (C3H/HeOu) mice with retinal degeneration, even when the gene therapy was performed early at postnatal day 24 (P24),[14] we quantified *Grm6* transcription in the retinas of *rd1* mice of up to 10 months of age by quantitative real-time PCR to ascertain whether *Grm6* expression was downregulated during the degenerative process. Thereby, we assumed that promoters active in the aggressive *rd1* photoreceptor degeneration mouse model are likely to be active in less severe degenerative models, as we have shown for the 4xGRM6-SV40 promoter, which is still active in the slower *rd10* (B6.CXB1-Pde6brd10) photoreceptor degeneration mouse line—but not in the *rd1* model—although with considerable off-target expression.[14]

We quantified *Grm6* transcription at P14, P21, P28, P54, and P318 in homogenized entire *rd1* retinas and determined *Grm6* transcription levels relative to transcription levels in wild-type C57BL/6 mouse retinas (n = 4, P54; Figure 2). Ribosomal protein L8 (*Rpl8*) was used as a reference gene, and *Rho* was used as marker for progressing photoreceptor degeneration. At P21, the relative *Rho* expression falls to 0.8% of its expression in adult C57BL/6 mice (Figure S1), consistent with severe rod photoreceptor loss. To compensate for the remaining photoreceptors in the early stages of degeneration that would bias toward an underestimation of *Grm6* levels compared to the levels in late stages, we normalized the measured *Grm6* transcription values against the remaining *Rho* transcription levels (Equation 3, in Materials and Methods). Figure 2 shows that the largest reduction in *Grm6*

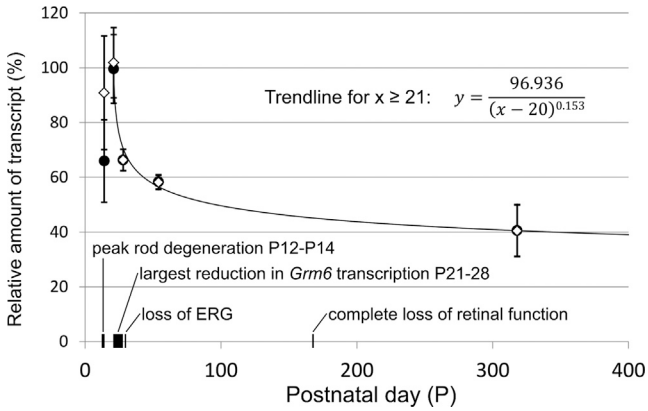

Figure 2. *Grm6* Transcription throughout Degeneration in the *rd1* Mouse Model

Grm6 transcription quantified by quantitative real-time PCR in whole *rd1* retinas (n = 6 at each time point) relative to *Grm6* transcripts in wild-type C57BL/6 mouse retinas (n = 4). Measured values (●); rod degeneration corrected values (◇). *Grm6* transcription starts decreasing beyond P21, following a power function, R^2 = 0.9866, and stabilizing around 40% of initial *Grm6* transcription in late degeneration. ERG, electroretinogram. Data are represented as mean ± SD of biological replicates.

transcription (−33.3%) takes place between P21 and P28, following the peak rod degeneration at P12–P14. Subsequently, *Grm6* transcript levels in the *rd1* retina stabilized at around 40% of the wild-type C57BL/6 level. This suggests that the silencing of 4xGRM6-SV40-driven expression in OBCs of the *rd1* mouse retina[14] was unlikely to be due to the *Grm6* enhancer. Having confirmed sustained *Grm6* transcription throughout the entire process of retinal degeneration, we chose the *GRM6* genome sequence as a template for synthetic promoter design.

Design of Short Human *GRM6*-Based Promoters

To optimally comply with the human transcription machinery, we based the promoter design on the human *GRM6* gene. To find potential regulatory genome sequences, we identified inter-species conserved DNA, active chromatin regions (DNase I hypersensitivity clusters or H3K27 acetylation), and potential transcription factor (TF) binding sites. The Gene Transcription Regulation Database (GTRD)[19,20] was used to retrieve chromatin immunoprecipitation DNA-sequencing (ChIP-seq) peaks, which provide experimentally verified TF binding sites.

To define the proximal promoter region, we focused on the 1,000 bp immediately 5′ of the translation start site (TLSS, defined as position 0; Figure 3A). When aligning the human and mouse sequences, we identified a 167-bp conserved sequence (−425 to −259; Figure 3A, striped region). We chose the first promoter variant, 566P (−691 to −126), to contain this 167-bp conserved sequence, the 3′ transcription start site (TSS; −179), and the 5′ H3K27Ac Mark signal peak (−656 to −405), as well as the potential binding site for the activating TF ERG. The second selected promoter variant, 454P (−453 to +1) also contains the full conserved 167-bp sequence but extends a further 3′ compared to 566P, reaching the translation start site (TLSS) and additionally containing the potential binding sites for the TFs MYC, POU5F1, and TCF7L1.

To select potential enhancer sequences, we focused on the human *GRM6* region around the sequence syntenic to the murine 200En *Grm6* enhancer previously identified by Kim and colleagues.[12] We identified a 310-bp-long sequence conserved between mouse and human genomes (−13,819 to −13,510) and extending beyond the murine 200En *Grm6* enhancer in both 3′ and 5′ directions (Figure 3B, striped section). We selected two enhancer variants, 407En and 770En. The short 407En enhancer (−13,873 to −13,467) contains the entire identified 310-bp conserved sequence. The longer 770En enhancer additionally contains all regulatory regions of interest in the 5′ direction, such as potential binding sites for the TFs DACH1, FLI1, and CTCF, as well as a DNase I hypersensitivity cluster (−13,990 to −13,816).

Evaluation of Promoters in the Human Retina

The human post-mortem retinal explant presents a valuable pre-clinical model for promoter testing; not only is it known that promoter activity and specificity vary largely among species,[9] but evaluation of promoter specificity also does not require a whole-eye *in vivo* gene therapy, since it is independent of the viral administration route.

For transduction of post-mortem human retinas, we cloned three *GRM6* enhancer/proximal promoter combinations (Table 2) upstream of the mCitrine reporter gene. We packaged expression constructs into the AAV2(7m8)[21] viral capsid, which is already being used for intravitreal injections into human eyes (ClinicalTrials.gov: NCT03326336). We used self-complementary (sc) AAV capsids that mediate faster gene expression (within approximately 1 week) compared to single-stranded (ss) AAVs (approximately 4–5 weeks), which is advantageous when working with *ex vivo* retinal cultures of limited longevity.

6×10^8–1.5×10^{10} vgs (vector genomes) were added to the ganglion cell side of cultured HREs at day 1. Explants were frozen and immunolabeled at day 8 of culture when mCitrine expression became detectable by eye (Figure S2). Cryosections were co-labeled with the nuclear stain DAPI to distinguish cell layers and antibodies against mCitrine (transgene) and Gao (OBC marker) to derive the identity of expressing [mCitrine+] cells. Photoreceptors are located in the outer nuclear layer (ONL), OBCs label positive for Gao and are located in the inner nuclear layer (INL), and ganglion cells are located in the ganglion cell layer (GCL) (Figures 4A and 4C). All three promoters—as opposed to highly unspecific transgene expression driven by 4xGRM6-SV40 (Figure S3)—showed high specificity for OBCs: 407En_454P(h*GRM6*) drove mCitrine expression in 83% ± 4% of OBCs, 407En_566P(h*GRM6*) drove expression in 75% ± 21% of OBCs, and 770En_454P(h*GRM6*) drove expression in 88% ± 13% of OBCs. To quantify promoter strength, we measured cytoplasmic Alexa 488 (secondary antibody for mCitrine) fluorescence in transduced OBC cell bodies (for details, refer to Materials and Methods). As evident from Figure 4B, promoters 770En_454P(h*GRM6*) (5.3 ± 1.3; n = 4; p = 0.002) and 407En_454P(h*GRM6*) (4.9 ± 0.2; n = 3;

p = 0.005) produced higher fluorescence values (FVs) than 407En_566P(h*GRM6*) (1.6 ± 0.2; n = 3), indicative of their superior performance in driving transgene expression.

For all subsequent experiments, we therefore used promoters with the promoter element 454P, which produced more efficient and stronger mCitrine expression.

Significantly Enhanced cOBC Preference in HREs

Currently, AAV gene therapies almost exclusively target the macula, the central area of the retina comprising the *fovea centralis*, which mediates high-acuity vision.[22] The ONL of the human *fovea* exclusively contains cones, which connect to cone bipolar cells in the inner retina forming the midget pathway underlying high-acuity vision. Fovea-targeted retinal gene therapy, therefore, demands a promoter that effectively drives expression in cOBCs.

To quantify selective expression in cOBCs, we performed triple labeling of human retinal cryosections with antibodies against the reporter protein mCitrine, Gao or Gy13 (ubiquitous OBC markers), and the rOBC cell-specific antibody protein kinase C alpha (PKCa) to distinguish rOBCs [PKCa+ and Gao+/Gy13+] and cOBCs [PKCa− and Gao+/Gy13+]. Figure 4C shows that 770En_454P(h*GRM6*) drives expression in both rOBCs and cOBCs. We counted mCitrine-expressing cOBCs as a fraction of all reporter-expressing OBCs and found that 770En_454P(h*GRM6*) drove expression in cOBCs at a higher ratio (22.3% ± 8.6%) compared to 407En_454P(h*GRM6*) (13.5% ± 1%). Since both promoters are active in rOBCs and cOBCs, the resulting expression ratio will always be influenced by the cOBC-to-rOBC ratio present in the transduced tissue, which varies in different retinal regions; the occurrence of cOBCs outside of the macula is low compared to the abundance of rOBCs.[23] To get a measure of the preference of a promoter for cOBCs, which is independent of the cOBC-to-rOBC ratio, we first calculated the expression efficacies for rOBCs and cOBCs separately (Equation 1).

$$\text{Expression efficacy (rOBCs)} = \frac{\text{expressing rOBCs [PKCa(+), Gao(+), mCitrine+]}}{\text{all rOBCs [PKCa(+), Gao(+)] in region}}$$

$$\text{Expression efficacy(cOBCs)} = \frac{\text{expressing cOBCs [PKCa(−), Gao(+), mCitrine+]}}{\text{all cOBCs [PKCa(−), Gao(+)] in region}}. \quad \text{(Equation 1)}$$

To get a measure for the absolute cOBC preference, independent of the retinal region, we then normalized cone-type expression efficacy to the local abundance of cones (Equation 2).

$$\text{cOBC preference(\%)} = \frac{\text{100 x expression efficacy(cOBC)}}{\text{expression efficacy(cOBC)} + \text{expression efficacy(rOBC)}}. \quad \text{(Equation 2)}$$

The cOBC preference of 770En_454P(h*GRM6*) was 48.2% ± 5.9%, indicating a virtually equal preference of the promoter for cOBCs and rOBCs. The cOBC preference of 770En_454P(h*GRM6*) was significantly higher (95% confidence interval [$CI_{95\%}$] of difference = 5.23–18.26, p = 0.004) than that of 407En_454P(h*GRM6*) (36.4% ± 2.3%; Figure 4D). To corroborate the excellent performance of 770En_454P(h*GRM6*) in cOBCs, we also cultured and transduced explants of human maculas where cOBCs largely predominate. As exemplified in Figure 5, 770En_454P(h*GRM6*) drove gene expression in macular cOBCs with high efficiency.

Transgene Expression Driven by Promoter 770En_454P(h*GRM6*) Is Independent of the Viral Capsid, Widespread, and Highly OBC Specific

To get a measure for the spread and distribution of expression produced by 770En_454P(h*GRM6*), we labeled transduced human retinal flat mounts with antibodies against mCitrine and Gao and determined the average amount of expressing OBCs on a large scale (Figure 6). We observed uniform mCitrine expression, targeting up to 82% of OBCs throughout the area of transduction (Figures 6A–6F). In particular, the efficacy of OBC-targeted mCitrine expression remained constant throughout the INL, regardless of depth (Figures 6C–6E), corroborating 770En_454P(h*GRM6*)'s equal preference for cOBCs (localized within the inner INL) and rOBCs (localized within the outer INL). To assess whether OBC specificity was influenced by the viral capsid, we compared mCitrine expression profiles produced by 770En_454P(h*GRM6*) side-by-side when packaged into scAAV2(7m8) and scAAV2(Y252,272,444,500,700,730F). The mutated variant AAV2(Y252,272,444,500,700,730F) was designed based on the findings of Petrs-Silva and colleagues[24] and was previously shown to transduce OBCs after intravitreal delivery in mice.[4] As shown in Figure 6G, the 770En_454P(h*GRM6*)-driven mCitrine

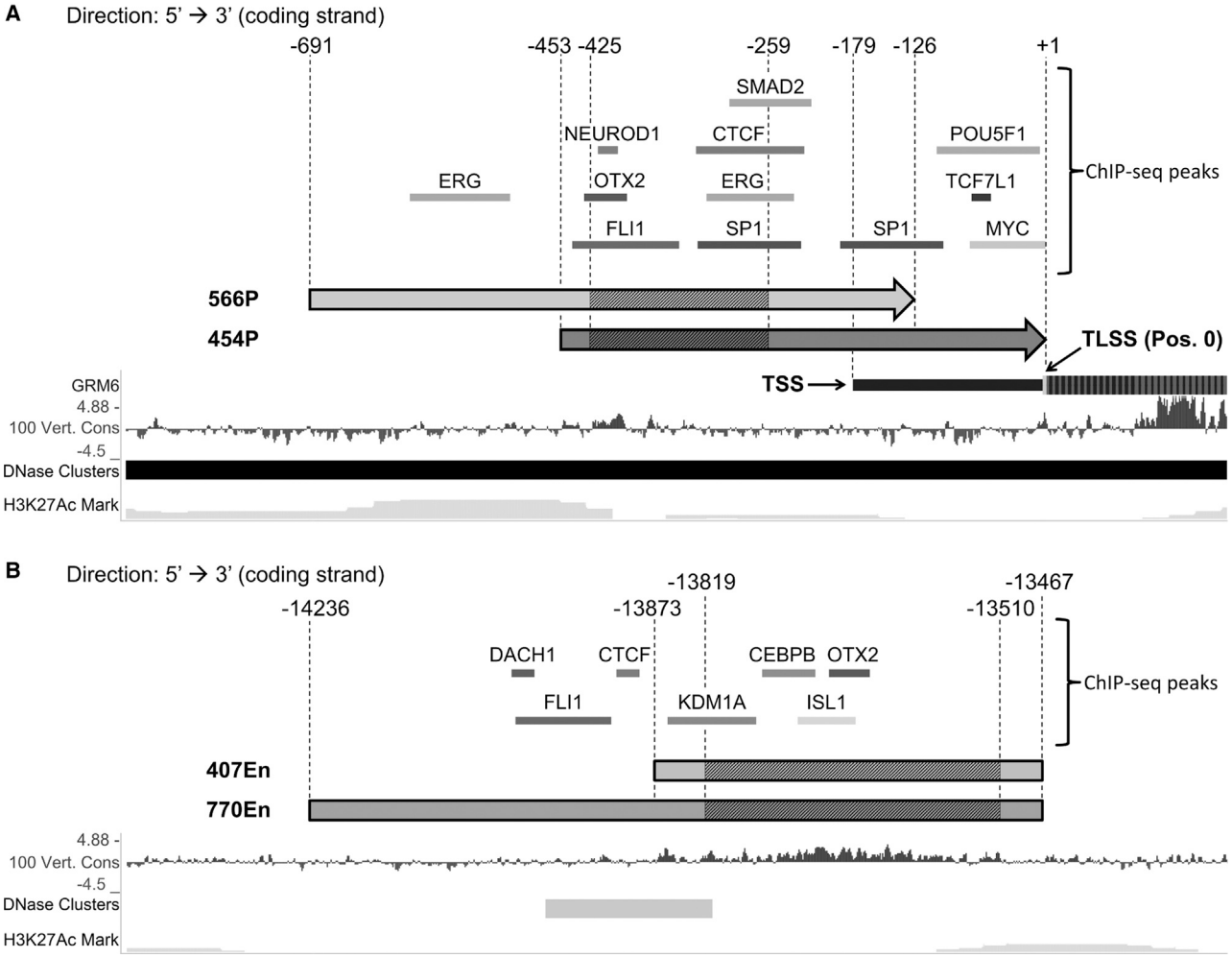

Figure 3. Design of Short Promoters based on Human *GRM6*

(A) Genomic region upstream of the translation start site (TLSS) showing the two selected proximal promoter variants, 566P and 454P. (B) Distal genomic region showing the two selected enhancer elements, 407En and 770En. Shaded regions indicate high sequence conservation between the murine and human genomes. Sequence locations are given relative to the TLSS. Markers for regulatory elements: DNase I hypersensitivity clusters, H3K27 acetylation marks, sequence conservation across 100 vertebrates (100 Vert. Cons) and ChIP-Seq peaks. TSS, transcription start site. Images were downloaded from the University of California, Santa Cruz (UCSC), Genome Browser at https://genome.ucsc.edu/ and modified.

expression profile was identical for both capsids, targeting equal levels of OBCs (scAAV2(7m8): 88.1% ± 13.1%, n = 3; scAAV2 (Y252,272,444,500,700,730F): 89.7% ± 3.5%; n = 3). Consequently, the high OBC specificity produced by 770En_454P(h*GRM6*) is a property of the promoter and independent of the AAV capsid.

Significant transgene expression in cells other than OBCs could lead to cytotoxicity and inflammatory reactions as well as to corrupt signaling in an optogenetic approach. Therefore, we quantified and compared OBC-specific and off-target transgene expression by measuring Alexa 488 fluorescence of the immunolabeled mCitrine reporter protein throughout the retina. Figure 6H shows that the normalized FVs in OBCs are significantly higher compared to those in other cells, which include ganglion cells, amacrine cells, photoreceptors, and OFF-type bipolar cells. Further, the equivalent FVs of rOBCs (5.4 ± 2.2) and cOBCs (5.2 ± 1.7) again confirmed equal functionality of 770En_454P(h*GRM6*) in both OBC types. In combination with the low off-target transduction rate (Figure 6G), we consider functional interference or induction of cytotoxic/inflammatory responses arising from off-target protein expression to be rather unlikely. To understand whether the ratio of off-target versus on-target expression is dependent on the viral dose applied, we correlated in different locations of the retinal explants OBC expression specificity and expression efficacy, the latter being directly dependent on the applied AAV dose (Figure S4). The correlation of specificity and efficacy was not significant ($p = 0.18$), from which we conclude that the OBC specificity of 770En_454P(h*GRM6*)-driven expression is independent of AAV dose.

Table 2. Selected Enhancer/Promoter Combinations

Name	GenBank identification	Length
407En_454P(h*GRM6*)	MT_212169	867 bp
407En_566P(h*GRM6*)	MT_212170	978 bp
770En_454P(h*GRM6*)	MT_212168	1243 bp

The combination of high OBC specificity and efficacy of expression driven by 770En_454P(h*GRM6*) allows for cell-type-specific intervention, maximizing functional outcome and reducing undesired side effects.

Optogenetic Vision Restoration with 770En_454P(h*GRM6*)-Driven OBC-Targeted Middle-Wave Opsin Expression in Fully Degenerated *rd1* Mouse Retinas

The tissue's accessibility to treatment is important for a retinal gene therapy. This can be challenging in a degenerative process accompanied by anatomical, functional, and transcriptional changes within the tissue.[25] HREs are not a degenerated tissue; therefore, we used the harsh photoreceptor degeneration *rd1* mouse model to test 770En_454P(h*GRM6*)'s performance in the degenerated retina. The 4xGRM6-SV40 promoter,[13] for example, was no longer functional in the OBCs of *rd1* mice when injected at 3.5 weeks of age and evaluated at 7.5 weeks of age.[14] To challenge the performance of 770En_454P(h*GRM6*), we performed an optogenetic gene therapy in late degenerated, 22-week-old *rd1* mice (n = 8). For this, we cloned an expression cassette in which promoter 770En_454P(h*GRM6*) drives the expression of murine medium-wave-sensitive cone opsin 1 (*Opn1mw*) and a red fluorescent protein (TurboFP635). We fused *Opn1mw* C-terminally with the entire C terminus of the OBC-specific mGluR6 receptor to achieve correct subcellular localization within the mGluR6 signalosome of the bipolar cell. We further added C-terminally a Golgi export signal (TS)[26] and the rhodopsin membrane trafficking sequence (TETSQVAPA) to improve membrane targeting. 770En_454P(h*GRM6*)-*Opn1mw*-CTmGluR6-TS-1D4-IRES2-TurboFP635 (Figure S5) was packaged into ssAAV2(7m8), and 1×10^{11} vgs were bilaterally and intravitreally injected. To ascertain functional *Opn1mw* expression, we quantified the visual acuity by detecting the optomotor response (OMR).[27] Briefly, the OMR of a mouse is a compensatory head movement reflex that serves the stabilization of a globally shifting visual image on the retina. By presenting to a mouse a laterally moving vertical black-and-white striped pattern, the highest spatial frequency that still elicits the OMR can be determined by stepwise increasing the spatial frequency of the pattern until the OMR is lost. The detection threshold can then be translated into the visual acuity of vision. We measured the OMR of the treated mice repeatedly between 28 and 38 weeks of age (n = 3). The average visual acuity of the treated mice was 0.28 ± 0.02 cycles per degree (cpd), which was significantly improved ($CI_{95\%}$ of difference = 0.087–0.237, p = 0.0001) compared to that of non-injected *rd1* littermates (0.12 ± 0.03 cpd; n = 5), reaching 65% of the values of seeing C57BL/6-positive controls (0.43 ± 0.05 cpd; n = 10; $CI_{95\%}$ of difference = 0.081–0.217, p = 0.0001) (Figure 7A). Importantly, restored visual acuity did not decrease over the 10-week test period (Figure S6), which is indicative of a halt or slowing down of retinal degeneration through optogenetic re-activation of inner retinal signaling. Mice were subsequently euthanized to visualize the retinal TurboFP635 expression pattern. Remarkably, transgene expression was found as virtually pan-retinal even in these very late degenerated retinas (*rd1*, 41 weeks of age: Figure 7B). Cryosections from additional treated *rd1* mice (n = 5) sacrificed at 26 weeks of age revealed that 770En_454P(h*GRM6*), in contrast to 4xGRM6-SV40, is able to drive *Opn1mw* expression also in OBCs of the degenerated retina with good expression efficacy (57.1% ± 4.3%; Figure 7C) and OBC specificity (59.1% ± 10%; Figure 7D). For comparison, expression specificity in wild-type C57BL/6 mice is higher (70.6% ± 5%; Figure S7), probably a consequence of transcriptomic changes during the process of degeneration.[14] Nonetheless, the good restoration of visual acuity in *rd1* mice confirms that the OBC specificity of 770En_454P(h*GRM6*) in *rd1* mice is still high enough to separate the retinal ON and OFF channels underlying contrast detection.

The extent to which degeneration will affect 770En_454P(h*GRM6*) promoter specificity in humans will need to be investigated, but widespread, cell-specific, functional, and stable therapeutic transgene expression in a degenerated retina well beyond any remaining retinal responsiveness or visual behavior (>24 weeks in *rd1* mice)[4,28] is, undoubtedly, a fundamental prerequisite for an effective gene therapy.

DISCUSSION

Retinal diseases are almost exclusively cell-type specific, and expression of a therapeutic gene in off- target cells was reported to enhance cytotoxic effects.[10] The challenge for gene therapy is, therefore, to achieve cell-type-specific transgene expression at functional levels. Such cell-type-specific treatment is, in particular, indispensable when optogenetic therapy is aimed at bipolar cells to restore complex and finely balanced inner retinal signaling between distinct retinal cell types. A further challenge is to achieve robust and specific transgene expression in degenerated tissue, since cellular transcriptomes often change in degeneration.[14] OBCs have proven particularly challenging target cells. Not only do they lie deep within the retina, making them less accessible to viruses, but they also appear rather non-permissive to viral transduction and require highly specialized promoters.[9]

Although murine OBCs were targeted with *Grm6*-derived promoters, albeit with varying specificity,[13,15,29] this success was not translated into human tissue (Figure S3) or late degenerated retinas.[14] The novel 770En_454P(h*GRM6*) promoter presented here paves the way for OBC-targeted human gene therapy. 770En_454P(h*GRM6*) not only targets a high percentage of OBCs throughout the human retina but also does this with a very high specificity for OBCs of approximately 90%. 770En_454P(h*GRM6*) also fulfills other requirements that render it well suited for a human retinal gene therapy: (1) it is sufficiently short (1,243 bp) to fit, together with a therapeutic transgene (i.e., an optogene), into an AAV capsid; (2) it is derived from the human genome and, therefore, optimally controlled by the human transcription machinery; (3) it possesses high functionality in the cOBCs,

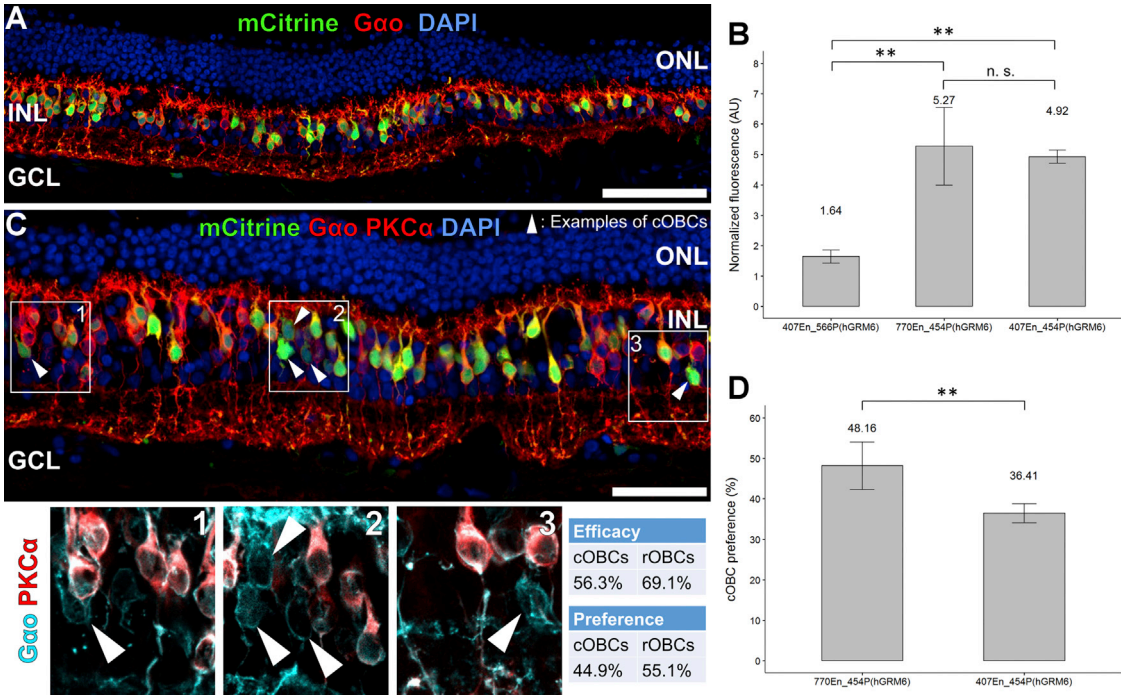

Figure 4. Functionality and ON-Bipolar Cell-Type Preference of Novel Synthetic Promoters in Post-mortem HREs

(A) Vertical cryosections through the mid-periphery of the human retina transduced with 770En_454P(h*GRM6*)-mCitrine. The nuclear stain DAPI differentiates the cell layers, the outer nuclear layer (ONL), the inner nuclear layer (INL), and the ganglion cell layer (GCL). In this example, 83% of ON-bipolar cells (OBCs) express the reporter mCitrine. Scale bar, 80 μm. (B) Quantification of the promoter strengths by measuring the fluorescence of immunolabeled mCitrine in expressing OBCs. Statistical analysis by one-way ANOVA with post hoc Tukey HSD test; $^{**}p < 0.01$; n.s., $p > 0.05$, not significant. (C) As in (A), but triple staining allowing distinction between rOBCs and cOBCs. In this example, 66% of OBCs express mCitrine. The magnified inserts show the differential labeling of rOBCs (Gao+, PKCa+) and cOBCs (Gao+, PKCa−). Expression efficacies, after Equation 1, and bipolar cell type preferences, after Equation 2, have been calculated for the given example. Scale bar, 50 μm. (D) Quantification of the overall cOBC preference of promoters 770En_454P(h*GRM6*) (n = 6) and 407En_454P(h*GRM6*) (n = 3). Statistical analysis by Welch's t test; $^{**}p < 0.01$. Data are represented as mean ± SD of biological replicates.

enabling macular OBC-targeted gene therapy for restoration of high-acuity vision; and (4) it drives expression at therapeutic levels also in degenerated tissue, leading to functional restoration. This was shown by the good restoration of the OMR in treated *rd1* mice with retinal degeneration, despite a significantly higher inner retinal off-target expression (27%) compared to HREs (5%). Reasons for the difference are potentially the human origin of the 770En_454P(h*GRM6*) promoter as well as the degenerative process, which is known to alter cellular transcriptomes;[14] corroborating the latter, we found that the inner retinal off-target expression of 770En_454P(h*GRM6*)-driven optogene expression in wild-type C57BL/6 mice is significantly lower (12.9% ± 4.8%; Figure S6) than in *rd1* mice (26.8% ± 7.2%, p = 0.0153; Figure 7D). Nonetheless, despite off-target expression of medium-wave cone opsin in cells other than OBCs, contrast sensitivity triggering the OMR was clearly restored, confirming successful re-establishment of the ON and OFF pathways emerging at the level of the bipolar cells.[30] Since OBC specificity of 770En_454P(h*GRM6*)-driven expression in HREs is very high (approximately 90%), it is expected that visual acuity will be reasonably well restored also in future human patients. Of course, off-target expression is relevant not only for optogenetic restoration but also for gene delivery in general, since significant transgene expression in cells other than OBCs could lead to cytotoxicity and inflammatory responses;[31] however, the number of expressing off-target cells is small compared to that of expressing OBCs, and transgene expression levels in off-target cells are significantly lower than those in OBCs (Figures 6G and 6H), rendering cytotoxic effects caused by off-target expression improbable.

AAV-mediated optogenetic gene therapy is, currently, the most promising approach to treat end-stage photoreceptor degenerative diseases of the retina independent of the underlying pathology, such as, for example, hereditary retinitis pigmentosa or geographic atrophy in late dry age-related macular degeneration. The two ongoing clinical trials by Allergan (ClinicalTrials.gov: NCT02556736) and GenSight Biologics (ClinicalTrials.gov: NCT03326336) target channelrhodopsins (ChR2[32] and ChrimsonR,[33] respectively) to the retinal ganglion cells. This will potentially restore luminance detection but with low visual acuity, since the diverse ganglion cell types (ON, OFF, transient, and sustained) will be engineered into one uniform response type, a sustained ON ganglion cell that starts firing action potentials when the light is turned on and stops signaling when light

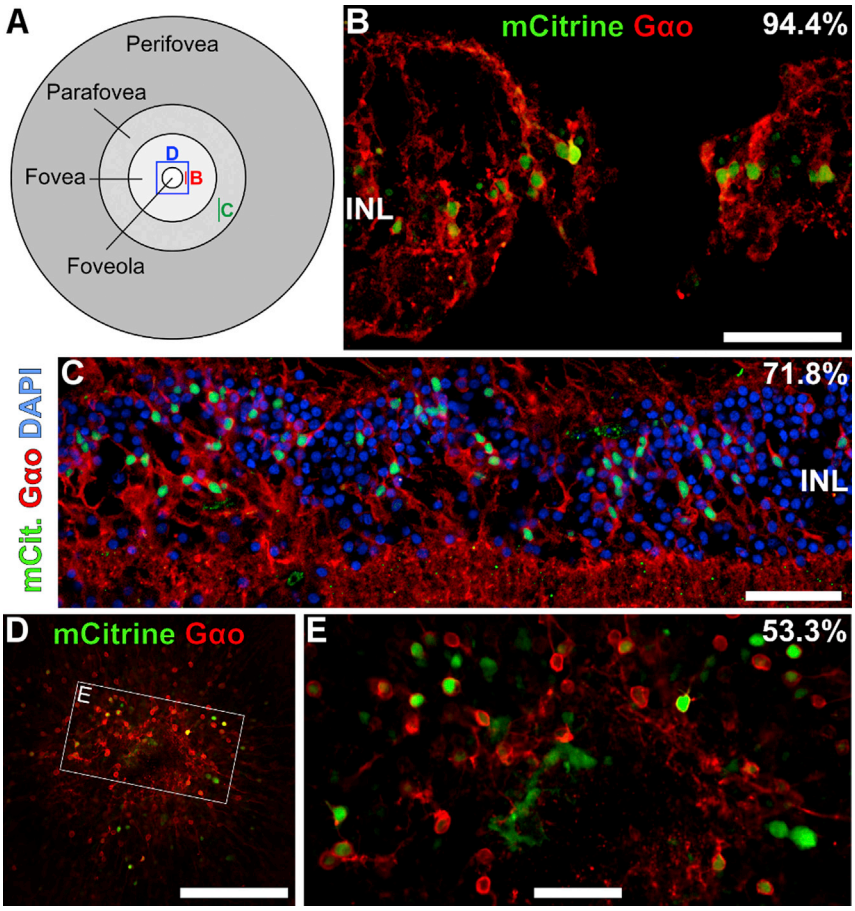

Figure 5. Promoter 770En_454P(h*GRM6*) Effectively Targets cOBCs of the Human Macula

(A) Terminology of macular areas with location of image acquisition indicated in (B)–(D). (B and C) Foveal (B) and para-foveal (C) sections. Scale bars, 50 μm. (D) Foveal flat mount. Scale bar, 200 μm. (E) Magnification of area indicated in (D). Scale bar, 50 μm. Local ON-bipolar cell expression efficacies are given in percentages. INL, inner nuclear layer.

is turned off. Use of 770En_454P(h*GRM6*), in contrast, enables optogenetic activation of OBCs and, with that, restoration of inner retinal signaling between bipolar, amacrine, and ganglion cells, which underlies high-level image formation, including contrast signaling and the detection of movement. Channelrhodopsins as therapeutic optogenetic tools potentially bear some disadvantages as well: they are of microbial origin, which may elicit an immunogenic response in a patient, and they require very high-activation light intensities, enhancing the risk of tissue phototoxicity in the treatment[34] and making the use of image processors necessary. To overcome the aforementioned potential drawbacks, research has started targeting OBCs with more refined, next-generation optogenetic tools based on human opsins, such as Opto-mGluR6[4] and rhodopsin.[6] Being G-protein-coupled receptors, these tools profit from an approximately 1,000-fold signal amplification mediated by the coupled intracellular G-protein cascade and endow OBCs with environmental light sensitivity.[4] Here, we expanded the set of OBC-targeted optogenetic strategies by implementing Opn1mw as a tool to render OBCs light sensitive. *Opn1mw* is expressed in green-light-sensitive cones, where it naturally couples to transducin, a G_i-type protein. Due to its G_i-type preference, Opn1mw has the ability to couple into the endogenous G_{io}-pathway of OBCs. We could demonstrate that 770En_454P(h*GRM6*)-driven, OBC-targeted *Opn1mw* expression restores the OMR at environmental illumination intensities (10^{13} photons cm^{-2} s^{-1}) in otherwise blind *rd1* mice. Notably, the restored discrimination of 0.28 cpd is substantially improved compared to values previously reported (0.056 cpd) for *rd1* mice treated by unspecific, hSyn-promoter-driven retinal *Opn1mw* expression.[35] This corroborates the importance of OBC-specific promoters for the restoration of high-acuity-pattern vision. It is also of note that we treated *rd1* mice at particularly late stages of degeneration (22 weeks of age), when neither retinal responsiveness nor visual behavior remained,[4,28] confirming the high functionality of promoter 770En_454P(h*GRM6*). Further, it was remarkable that the quality of restored visual acuity persisted robustly throughout the testing period and up to 10 months of age, indicative of a stabilization of inner retinal degeneration possibly due to the re-activation of retinal light signaling. All the aforementioned data are fundamental for a durable treatment of a human patient where the diagnosis of vision loss typically takes place during the late stages of degeneration.

Besides optogenetic therapies, OBC-targeted gene supplementation therapies with the potential of treating CSNB will also profit from 770En_454P(h*GRM6*). Most forms of CSNB are caused by mutations within OBC-expressed genes such as *NYX*, *GRM6*, *TRPM1*, *GPR179*, *GNB3*, and *LRIT3*, which encode proteins involved in the OBC-signaling cascade[8] (Figure 1B). Preclinical endeavors are underway that supply a functional version of the mutated gene to the OBCs to restore the mGluR6 signaling pathway and, with that, OBC function and vision.[18] In terms of translation into the clinics and testing in human subjects, we see no major challenge for 770En_454P(h*GRM6*). Regarding safety, 770En_454P(h*GRM6*) consists of entirely human DNA elements. In terms of efficacy, mCitrine expression was visible by eye already 7 days post-transduction, and sufficient OPN1mw was expressed in the *rd1* mouse retina to restore a solid OMR; however, the efficacy of expressing larger, more complicated proteins, such as membrane proteins—in particular, optogenetic proteins—in the human retina remains to be

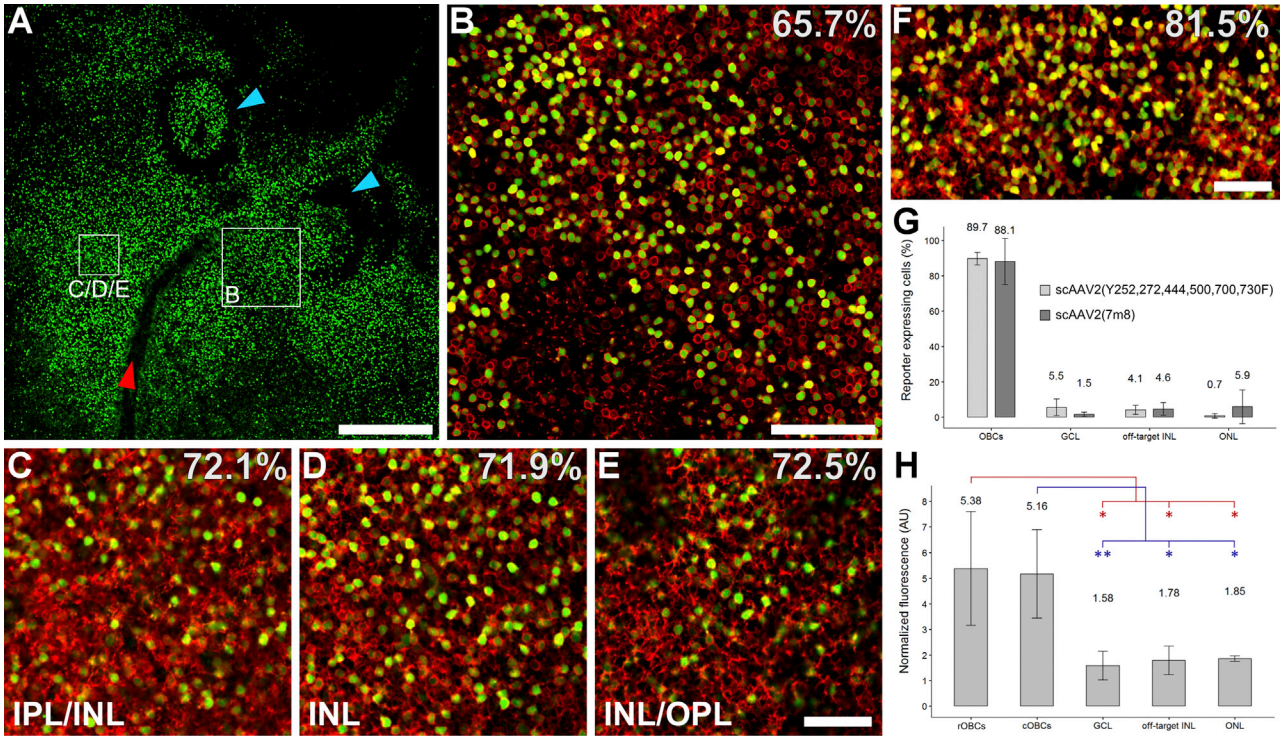

Figure 6. Capsid-Independent and Widespread ON-Bipolar Cell-Specific Expression Driven by Promoter 770En_454P(h*GRM6*) in HREs

(A) Flat mount transduced with scAAV2(7m8)-770En_454P(h*GRM6*)-mCitrine, with the application site indicated with blue arrowheads pointing toward pipette marks. mCitrine indicates that the drop of viral solution remained locally at the application site and, consequently, accessed the inner nuclear layer (INL) predominantly through the inner limiting membrane. Red arrowhead indicates blood vessel. Scale bar, 500 μm. (B–F) The ON-bipolar cell (OBC) expression efficacy, given in percentages, remained approximately constant throughout the explant (B–E), throughout the inner edge (C), middle (D) and outer edge (E) of the INL, and in explants from different donors (A–E versus F). IPL, inner plexiform layer; OPL, outer plexiform layer. Scale bars: 100 μm in (B) and 50 μm in (C)–(F). Staining in (B)–(F) was done with anti-Gao and anti-mCitrine. (G) Transduction fingerprint shown to be independent of the viral capsid used. AAV2(7m8) (n = 3) and AAV2(Y252,272,444,500,700,730F) (n = 3) produced virtually identical expression profiles with a high OBC specificity of ~88%. Off-target INL includes OFF-bipolar cells and amacrine cells. GCL, ganglion cell layer; ONL, outer nuclear layer. (H) Somatic fluorescence intensities produced by 770En_454P(h*GRM6*) quantified in immunolabeled cryosections (n = 3). The fluorescence intensities in rOBCs and cOBCs were significantly higher than the intensities in off-target populations. Statistical analysis by one-way ANOVA with post hoc Tukey HSD test: *$p < 0.05$; **$p < 0.01$. Data are represented as mean ± SD of biological replicates.

tested. In terms of manufacturing, which mainly concerns the AAV capsid and not the transgene, we foresee no issues for 770En_454P(h*GRM6*), since it complies in size with other promoters used in ssAAV gene therapy.

The center of the human retina (*fovea centralis*), which mediates high-acuity vision, and the surrounding central retina, the macula, are understandably the primary focus of current retinal gene therapies.[22] Promoter 770En_454P(h*GRM6*) empowers OBC-targeted macular gene therapies with the promise to restore high-quality vision. In age-related macular degeneration, Stargardt disease, and cone-rod dystrophies, the macular cones are primarily affected.[36] The macula, however, is also affected in later stages of rod-cone dystrophies, such as hereditary retinitis pigmentosa.[37] Subretinal injections typically place AAVs close to the central retina. Intravitreal injections currently also only lead to transgene expression within the macula of primates and probably also humans.[38,39] The reason is 2-fold: first, only in the macular region is the inner limiting membrane barrier thin enough to allow viral particles to pass. Second, the bipolar and ganglion cells connecting to the foveal cones are laterally pushed aside from the fovea, rendering them directly accessible from the vitreous.[16,40] Of course, endeavors are being made to achieve pan-retinal transduction, such as multifocal subretinal injections, inner limiting membrane peeling before intravitreal injection,[38] and AVV engineering for improved penetration of the inner limiting membrane.[21] Despite the unarguable importance of the macula as a target for gene therapy, transduction of macular OBCs has, however, not yet been achieved. This is because the macula is dominated by the cOBCs, which remained, until the development of 770En_454P(h*GRM6*), inaccessible to transgene expression. The reason for this may be that cOBCs require particularly specialized promoters. Which elements of 770En_454P(h*GRM6*) then could convey the high functionality in the cOBCs? cOBC functionality

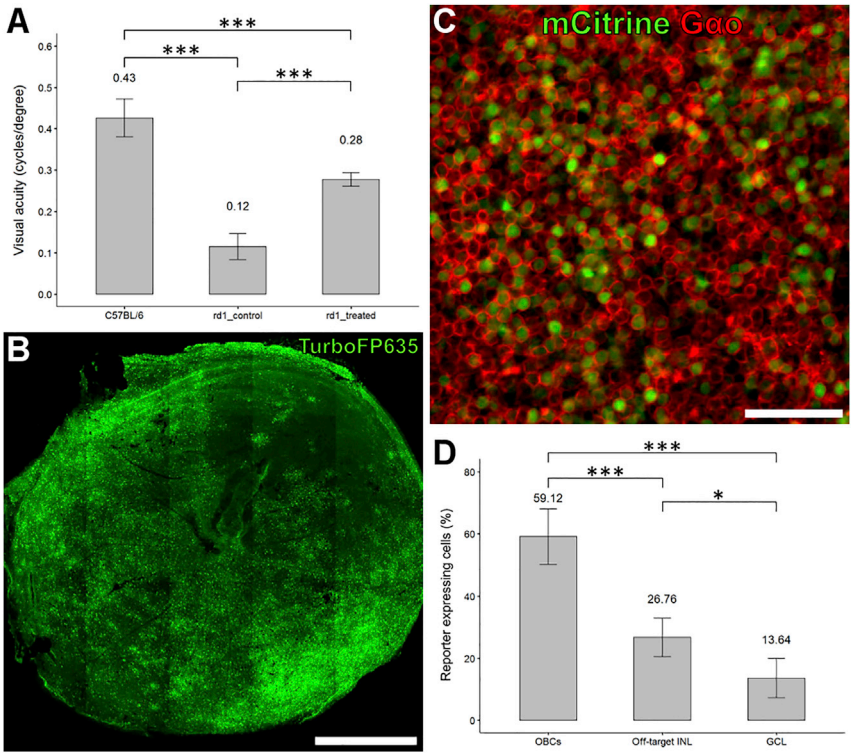

Figure 7. Promoter 770En_454P(h*GRM6*) Drives Stable, Functional, and Widespread *Opn1mw* Expression in Late Degenerated *rd1* Mice

(A) AAV2(7m8)-770En_454P(h*GRM6*)-*Opn1mw*-IRES2-TurboFP635-injected *rd1* mice were tested for visual acuity determined by the optomotor reflex between 28 and 38 weeks of age (n = 3) and compared to their untreated littermates (n = 5). Optogenetically treated mice showed significant restoration of visual acuity with a restoration of 65% of the visual acuity of wild-type mice (C57BL/6; n = 10). (B and C) Retinas of the treated animals were immunohistochemically evaluated for their expression profiles, as indicated in the whole mounts of (B) at 41 weeks of age and (C) at 26 weeks of age. Scale bars: 1,000 μm in (B) and 50 μm in (C). (D) 770En_454P(h*GRM6*) had a significant specificity for ON-bipolar cells (OBCs) also in late degenerated tissue at 26 weeks of age. INL, inner nuclear layer; GCL, ganglion cell layer. Statistical analysis by one-way ANOVA with post hoc Tukey HSD test: *$p < 0.05$; ***$p < 0.001$. Data are represented as mean ± SD of biological replicates.

could be mediated through (1) the proximal promoter element (2), the enhancer element, and (3) the distance and interaction between transcription factor binding sites in the enhancer and the proximal promoter. The more effective promoter element 454P contains additional binding sites for the transcriptional regulators TCF7L1 (regulator of Wnt signaling),[41] MYC (highly pleiotropic transcription factor),[42] and POU5F1 (involved in embryonic development and stem cell pluripotency;[43] Figure 3A). Additionally, in promoter variants containing 454P(h*GRM6*), the distance between TF binding sites in the enhancer and the proximal promoter is reduced, which was previously linked to enhanced promoter functionality.[15] The observed difference in terms of cOBC preference between promoters 770En_454P(h*GRM6*) and 407En_454P(h*GRM6*) must lie in the enhancer element 770En. The 5′ region of 770En contains additional binding sites for CTCF (transcriptional and epigenetic regulation),[44] DACH1 (transcriptional regulator implicated in neural development),[45,46] and FLI1 (activator, proto-oncogene),[47] which may all be involved in the enhancement of activity. Since FLI1 is known to homodimerize with itself and hetero-dimerize with ERG,[48] DNA looping through binding with FLI1 and ERG contained in the proximal promoter may approximate enhancer and promoter, which may potentially enhance functionality in cOBCs. Indeed, a recent study described a synergistic role of FLI1 and ERG in the gene regulation of endothelial cells.[49]

Besides leveraging OBC-targeted clinical gene supplementation and optogenetic gene therapies with the potential to restore high-acuity vision, 770En_454P(h*GRM6*) also empowers basic research, for the first time permitting controlled manipulation of OBC activity across species. This will contribute to ongoing revelations of the still rather elusive inner retinal signaling, not only in health but, importantly, also in degenerated retinal tissue. These insights can, in turn, serve as an exemplar for other degenerating neuronal networks. In summary, promoter 770En_454P(h*GRM6*) mediates highly OBC-specific, robust, and durable transgene expression, even in the late degenerated retina and possesses the unique ability to effectively drive transgene expression in cOBCs resident in the human fovea and mediating high-acuity vision.

MATERIALS AND METHODS

Bioinformatic Analysis and Promoter Design

We obtained genomic sequences and information on DNase I clusters, H3K27Ac marks, and cross-species conservation for *GRM6* and *Grm6* from the Genome Browser of the Genomics Institute of the University of California, Santa Cruz (https://genome.ucsc.edu/, assemblies GRCh37/hg19, GRCh38/hg38, and GRCm38/mm10).[50,51] We retrieved ChIP-seq data from the Gene Transcription Regulation Database (http://gtrd.biouml.org/)[19,20] and performed sequence alignments online with "blastn" (https://blast.ncbi.nlm.nih.gov/Blast.cgi).[52,53]

Quantitative Real-Time PCR of *Grm6* Transcription

isolated RNA with the SV Total RNA Isolation System (Promega, Z3100) from the pooled retinas of each mouse and performed quantitative real-time PCRs in duplicates with the Luna Universal One-Step RT-qPCR Kit (New England Biolabs, E3005) using KiCqStart SYBR Green Primers (KSPQ12012G) for *Grm6*, *Rho*, and the reference gene *Rpl8*. We used Equation 3 to mitigate the

underestimation of *Grm6* transcription levels in the early stages of degeneration.

$$\mathrm{Va}(Grm6, \mathrm{x}) = \mathrm{Vm}(Grm6, \mathrm{x}) \times \left[\#\mathrm{rods} \times \frac{\mathrm{Vm}(Rho, \mathrm{x})}{\mathrm{Vm}(Rho,\ \mathrm{C57BL6J})} + \#(\text{other cells})\right], \quad \text{(Equation 3)}$$

where Va stands for value adjusted, Vm stands for value measured, and x stands for the time point in degeneration; #rods represents the average amount of rods (6.4 Mio),[54] and #(other cells) represents the average amount of non-rod cells (1.678 Mio)[54,55] in a healthy mouse retina. The adjustment is an estimate that assumes that the effect of changing non-rod cell numbers during degeneration is negligible. We further normalized the adjusted and measured values to the respective values of the wild-type animals.

Promoter Cloning and Viral Vectors

We isolated human genomic DNA from blood with the NucleoSpin Blood Kit (Macherey-Nagel, 740951). We PCR-amplified *GRM6* enhancer and proximal promoter sequences, combined them into synthetic promoters, and then cloned the promoters into AAV plasmids. For HRE experiments, we used the scAAV plasmid pAAVsc_U7DTex23[56] (a kind gift by P. Odermatt and L. Garcia) as the backbone. To clone the synthetic promoters upstream of reporter mCitrine, followed by the woodchuck hepatitis virus posttranscriptional regulatory element (WPRE) and the short polyadenylation signal sNRP1-pA,[57] we PCR-amplified XbaI-NheI-MfeI-MfeI-AgeI-Kozak-mCitrine-WPRE-sNRP-1 pA-MluI from plasmid pAAV-4xGRM6-SV40_Opto-mGluR6_IRES_mCitrine_WPRE_BGH pA[14] and inserted it into pAAVsc_U7DTex23 using restriction sites XbaI and MluI. Into this new backbone, we then inserted the synthetic promoters upstream of mCitrine by restriction with EcoRI/MfeI (compatible cohesive ends) and AgeI for 407En_454P(h*GRM6*) and 407En_566P(h*GRM6*), or restriction with XbaI and AgeI for 770En_454P(h*GRM6*) (Figure S8). For mouse experiments, we cloned the plasmid backbone pAAV-4xGRM6-SV40_Opto-mGluR6_IRES_TruboFP635_WPRE_BGH pA as described by van Wyk et al.[14] but with TurboFP635 instead of mCitrine. Then, we PCR-amplified *Opn1mw* from murine retinal cDNA (GoScript Reverse Transcriptase, Promega), replacing the stop codon with the entire C terminus of mGluR6 followed by a Golgi export signal (TS)[26] and the rhodopsin trafficking sequence (TETSQVAPA, 1D4 epitope). We subsequently replaced 4xGRM6-SV40_Opto-mGluR6 in the plasmid backbone by using adaptor PCR and the In-Fusion HD Cloning Plus Kit (Takara, 638909). We again used adaptor PCR to then insert 770En_454P(h*GRM6*) upstream of *Opn1mw*, resulting in ssAAV plasmid pAAV-770En_454P(h*GRM6*)-*Opn1mw*-CTmGluR6-TS-1D4-IRES2-TurboFP635-WPRE-BGHpA (Figure S5). We packaged viral vectors with capsids AAV2(7m8)[21] andAAV2(Y252,272,444,500,700,730F)[4,24] as described elsewhere.[14] Vector NTI Advance was used for generating plasmid maps.

Mouse Injections

We obtained C57BL/6J and C3H/HeOuJ (*rd1*) mice from breeding stocks at the Jackson Laboratory (Bar Harbor, ME, USA). Mice were kept and bred under standard conditions and according to legal requirements. The Swiss Veterinary Office reviewed and approved all animal experiments and procedures. The same skilled person performed all intravitreal injections as described elsewhere.[14]

HRE Cultures and Viral Transduction

All procedures were in accordance with the tenets of the Declaration of Helsinki and complied with governmental regulations. No ethics approval was required for this study as per national laws and regulations (Federal Act on Research involving Human Beings [Human Research Act, HRA 810.30, Art. 38]), and the Swiss Ethics Committee reviewed this study and exempted it from the ethics review process. The anonymized donor tissue was provided by the Department of Ophthalmology, Inselspital, Bern University Hospital, Bern, Switzerland. We prepared and handled HREs as previously described.[14] In short: we prepared HREs of approximately 50 mm^2 from the mid-periphery (8–15 mm distal from the macula) of the retina or from the macula 3–24 h post-mortem and cultured them in R16 medium with supplements.[58] To prevent the virus from flowing into the culturing medium, we placed a small volume (3 μL) of viral solution directly onto the ganglion cell side of the retina, in the middle of the explant. We processed HREs for immunohistochemistry after 7 days in culture.

Immunohistochemistry

We fixed mouse retinas, after enucleation and removal of the cornea and lens, for 2 h and human retinas for 30 min in 4% paraformaldehyde (PFA) and subsequently cryo-protected them in a sucrose gradient (10%, 20%, and 30% (wt/wt) sucrose in PBS) for a minimum of 2 h at each concentration. For cryosectioning, we embedded retinas with Tissue-Tek O.C.T. Compound (Sakura Finetek) in cryomolds, froze them in liquid-nitrogen-cooled 2-methylbutane, cut them into vertical cryo-sections of 15-μm thickness on a cryostat (Leica), and mounted them on SuperFrost Ultra Plus Adhesion slides (Thermo Scientific). We used 2xNGS (Sigma-Aldrich, G9023) and 2xNDS (Sigma-Aldrich, D9663) (6% normal serum, 2% BSA, and 0.3% Triton X-100 in 1× PBS) and prepared antibody solutions (AB solutions) (Table S1) in 1× blocking solution (mixed 1:1 with 1× PBS). After 1 h of blocking, we incubated slides in primary AB solution overnight at 4°C and subsequently in secondary AB solution with DAPI (0.65 μg/mL, Sigma-Aldrich) for 2 h at room temperature. For the triple staining with anti-Gao, we used a sequential staining protocol: We first stained against PKCa and mCitrine as described earlier and then incubated the sections with anti-Gao for 2 h at room temperature and subsequently with anti-Mouse Cyanine 5 for another 2 h at room temperature. For staining of whole mounts or flat mounts, we blocked samples in blocking solution overnight and incubated in primary AB solution for 6 days at 4°C and in secondary AB solution for 5 days at 4°C. Finally we mounted the stained samples on glass slides with Fluoromount mounting medium (Sigma-Aldrich, F4680).

Microscopy and Quantitative Fluorescence Measurements

We used a ZEISS LSM 880 with Airyscan and ZEN 2.1 software and either a Plan-Apochromat 20×/0.8 M27 or a Plan-Apochromat 40×/1.3 Oil DIC M27 objective lens and performed image processing and evaluation in Fiji. We measured FVs in different areas of immunolabeled cryo-sections by selecting cell bodies with the freehand selection tool of Fiji and measuring the average FV of Alexa 488-labeled mCitrine with the "analyze-measure" command. We treated samples as identically as possible but normalized the median of measured FVs to the background fluorescence in untransduced OBCs to compensate for remaining experimental variations. For better comparison, we also normalized the fluorescence intensities measured in the triple-stained sections to the intensities measured in the double-stained sections. The total number of cells measured for FVs or counted for cell-type specificity quantification is given in Table S2.

Optomotor Reflex Measurements

We measured visual acuity by OMRs in the OptoDrum (Striatech) virtual optomotor system. It contained a small chamber (54 × 54 × 30 cm) with four screens (23.8", 1920x1080 pixel resolution, in-plane switching [IPS] screen) surrounding a platform. The brightness of the screens was adjusted to 10^{13} photons cm^{-2} s^{-1}, and the bottom and the top of the chamber were covered with mirrors. Head movements of unrestrained mice sitting on an elevated platform (9-cm diameter, 10-cm height) were tracked from above by an infrared-sensitive digital camera (1/3" complementary metal oxide semiconductor (CMOS) sensor with global shutter and wide-angle lens, F1.6) while a rotating pattern of black and white vertical bars was displayed at different spatial frequencies controlled by the software. The velocity of the moving bars was set to 12°/s, and the contrast was set to 100%. Optodrum software analyzed the recorded head movements, evaluated whether the mice followed the stimulus pattern, and rated the trial as positive or negative. Visual acuity of optogenetically treated *rd1* mice at different time points in degeneration were not significantly different (ANOVA, $p = 0.214$; $CI_{95\%}$ of difference for weeks 33–28 = [−0.091, 0.209]; $CI_{95\%}$ of difference for weeks 38–28 = [−0.2, 0.1]; $CI_{95\%}$ of difference for weeks 38–33 [−0.293, 0.074]; Figure S6); therefore, we used the averages of the trials of individual mice for comparisons with positive and negative controls.

Statistics

We performed statistical tests in R v.3.6.0.[59] We used one-way ANOVA for multiple comparisons with post hoc analysis with Tukey's honestly significant difference (HSD). We used Welch's t test for comparisons between two populations. Assumptions of normality were not rejected by the Shapiro-Wilk normality test, and assumptions of homoscedasticity were not rejected by Levene's test for homogeneity of variance. In graphs, the significance levels are indicated as $p \leq 0.05$, $p \leq 0.01$, and $p \leq 0.001$. Values are given as the mean ± standard deviation of biological replicates.

We performed power calculations with the pwr.anova.test function to estimate the required sample size for all experiments comparing synthetic promoter variants and the different treatment groups in optomotor reflex measurements. We estimated standard deviations (SDs) through pilot experiments (HRE experiments) or with values reported in the literature[28] (OMR): SD for cOBC preference, 4.8%; SD for normalized fluorescence, 1.09; and SD for visual acuity, 0.04 cpd. We anticipated the following differences between group means to be scientifically meaningful and functionally relevant: cOBC preference, 10%; normalized fluorescence, 2.4 (50% of the mean of the pilot experiment); and visual acuity, 0.1 cpd. Dividing these in-between group mean differences by the respective SDs, we calculated the following effect sizes; cOBC preference, 2.083; normalized fluorescence, 2.213; and visual acuity, 2.5. We performed power calculations for an ANOVA of 3 groups (for the three synthetic promoters 407En_454P(h*GRM6*), 407En_566P(h*GRM6*), and 770En_454P(h*GRM6*) or 3 groups of mice in the OMR experiments) at a significance level of 0.05 and power of 0.9, which all yielded necessary biological sample sizes of between 2 and 3.

SUPPLEMENTAL INFORMATION

Supplemental Information can be found online at https://doi.org/10.1016/j.omtm.2020.03.003.

AUTHOR CONTRIBUTIONS

E.C.H. performed the great majority of experiments; S.M.H. performed the OMR experiments; and S.K. funded the project, wrote the paper, and drafted the project and experiments.

CONFLICTS OF INTEREST

The authors declare no competing interests.

ACKNOWLEDGMENTS

We would like to thank Michiel van Wyk for performing the intravitreal injections, for the many fruitful discussions and experimental support, and for editing the manuscript. We also thank Sabine Schneider and Lara Girod for virus packaging and help with cloning and quantitative real-time PCR, Pascal Escher for useful tips on quantitative real-time PCR, Nino Stocker for help with immunohistochemistry, Volker Enzmann for the access to human donor eyes, Yvan Arsenijevic for his donation of basal R16 medium powder, and Michael Känzig for taking care of the animal facility. We thank the Swiss National Science Foundation (31003A_152807 and 31003A_176065), the Bertarelli Foundation (Catalyst fund, project BCL7O2), Haag-Streit Holding, and Arctos Medical for the funding of this project.

REFERENCES

1. Trapani, I., and Auricchio, A. (2019). Has retinal gene therapy come of age? From bench to bedside and back to bench. Hum. Mol. Genet. *28* (R1), R108–R118.
2. Gollisch, T., and Meister, M. (2010). Eye smarter than scientists believed: neural computations in circuits of the retina. Neuron *65*, 150–164.
3. Burkhardt, D.A. (2011). Contrast processing by ON and OFF bipolar cells. Vis. Neurosci. *28*, 69–75.
4. van Wyk, M., Pielecka-Fortuna, J., Löwel, S., and Kleinlogel, S. (2015). Restoring the ON-switch in blind retinas: Opto-mGluR6, a next-generation, cell-tailored optogenetic tool. PLoS Biol. *13*, e1002143.

5. Lagali, P.S., Balya, D., Awatramani, G.B., Münch, T.A., Kim, D.S., Busskamp, V., Cepko, C.L., and Roska, B. (2008). Light-activated channels targeted to ON bipolar cells restore visual function in retinal degeneration. Nat. Neurosci. *11*, 667–675.

6. Cehajic-Kapetanovic, J., Eleftheriou, C., Allen, A.E., Milosavljevic, N., Pienaar, A., Bedford, R., Davis, K.E., Bishop, P.N., and Lucas, R.J. (2015). Restoration of vision with ectopic expression of human rod opsin. Curr. Biol. *25*, 2111–2122.

7. Gaub, B.M., Berry, M.H., Holt, A.E., Reiner, A., Kienzler, M.A., Dolgova, N., Nikonov, S., Aguirre, G.D., Beltran, W.A., Flannery, J.G., and Isacoff, E.Y. (2014). Restoration of visual function by expression of a light-gated mammalian ion channel in retinal ganglion cells or ON-bipolar cells. Proc. Natl. Acad. Sci. USA *111*, E5574–E5583.

8. Martemyanov, K.A., and Sampath, A.P. (2017). The transduction cascade in retinal ON-bipolar cells: signal processing and disease. Annu. Rev. Vis. Sci. *3*, 25–51.

9. Jüttner, J., Szabo, A., Gross-Scherf, B., Morikawa, R.K., Rompani, S.B., Hantz, P., Szikra, T., Esposti, F., Cowan, C.S., Bharioke, A., et al. (2019). Targeting neuronal and glial cell types with synthetic promoter AAVs in mice, non-human primates and humans. Nat. Neurosci. *22*, 1345–1356.

10. Xiong, W., Wu, D.M., Xue, Y., Wang, S.K., Chung, M.J., Ji, X., Rana, P., Zhao, S.R., Mai, S., and Cepko, C.L. (2019). AAV *cis*-regulatory sequences are correlated with ocular toxicity. Proc. Natl. Acad. Sci. USA *116*, 5785–5794.

11. Siegert, S., Cabuy, E., Scherf, B.G., Kohler, H., Panda, S., Le, Y.Z., Fehling, H.J., Gaidatzis, D., Stadler, M.B., and Roska, B. (2012). Transcriptional code and disease map for adult retinal cell types. Nat. Neurosci. *15*, 487–495, S1–S2.

12. Kim, D.S., Matsuda, T., and Cepko, C.L. (2008). A core paired-type and POU homeodomain-containing transcription factor program drives retinal bipolar cell gene expression. J. Neurosci. *28*, 7748–7764.

13. Cronin, T., Vandenberghe, L.H., Hantz, P., Juttner, J., Reimann, A., Kacsó, A.E., Huckfeldt, R.M., Busskamp, V., Kohler, H., Lagali, P.S., et al. (2014). Efficient transduction and optogenetic stimulation of retinal bipolar cells by a synthetic adeno-associated virus capsid and promoter. EMBO Mol. Med. *6*, 1175–1190.

14. van Wyk, M., Hulliger, E.C., Girod, L., Ebneter, A., and Kleinlogel, S. (2017). Present molecular limitations of ON-bipolar cell targeted gene therapy. Front. Neurosci. *11*, 161.

15. Lu, Q., Ganjawala, T.H., Ivanova, E., Cheng, J.G., Troilo, D., and Pan, Z.H. (2016). AAV-mediated transduction and targeting of retinal bipolar cells with improved mGluR6 promoters in rodents and primates. Gene Ther. *23*, 680–689.

16. Ramachandran, P.S., Lee, V., Wei, Z., Song, J.Y., Casal, G., Cronin, T., Willett, K., Huckfeldt, R., Morgan, J.I., Aleman, T.S., et al. (2017). Evaluation of dose and safety of AAV7m8 and AAV8BP2 in the non-human primate retina. Hum. Gene Ther. *28*, 154–167.

17. Santos, A., Humayun, M.S., de Juan, E., Jr., Greenburg, R.J., Marsh, M.J., Klock, I.B., and Milam, A.H. (1997). Preservation of the inner retina in retinitis pigmentosa. A morphometric analysis. Arch. Ophthalmol *115*, 511–515.

18. Scalabrino, M.L., Boye, S.L., Fransen, K.M., Noel, J.M., Dyka, F.M., Min, S.H., Ruan, Q., De Leeuw, C.N., Simpson, E.M., Gregg, R.G., et al. (2015). Intravitreal delivery of a novel AAV vector targets ON bipolar cells and restores visual function in a mouse model of complete congenital stationary night blindness. Hum. Mol. Genet. *24*, 6229–6239.

19. Yevshin, I., Sharipov, R., Valeev, T., Kel, A., and Kolpakov, F. (2017). GTRD: a database of transcription factor binding sites identified by ChIP-seq experiments. Nucleic Acids Res. *45* (D1), D61–D67.

20. Yevshin, I., Sharipov, R., Kolmykov, S., Kondrakhin, Y., and Kolpakov, F. (2019). GTRD: a database on gene transcription regulation-2019 update. Nucleic Acids Res. *47* (D1), D100–D105.

21. Dalkara, D., Byrne, L.C., Klimczak, R.R., Visel, M., Yin, L., Merigan, W.H., Flannery, J.G., and Schaffer, D.V. (2013). In vivo-directed evolution of a new adeno-associated virus for therapeutic outer retinal gene delivery from the vitreous. Sci. Transl. Med. *5*, 189ra76.

22. Provis, J.M., Dubis, A.M., Maddess, T., and Carroll, J. (2013). Adaptation of the central retina for high acuity vision: cones, the fovea and the avascular zone. Prog. Retin. Eye Res. *35*, 63–81.

23. Volland, S., Esteve-Rudd, J., Hoo, J., Yee, C., and Williams, D.S. (2015). A comparison of some organizational characteristics of the mouse central retina and the human macula. PLoS ONE *10*, e0125631.

24. Petrs-Silva, H., Dinculescu, A., Li, Q., Deng, W.T., Pang, J.J., Min, S.H., Chiodo, V., Neeley, A.W., Govindasamy, L., Bennett, A., et al. (2011). Novel properties of tyrosine-mutantAAV2 vectors in the mouse retina. Mol. Ther. *19*, 293–301.

25. Jones, B.W., Pfeiffer, R.L., Ferrell, W.D., Watt, C.B., Marmor, M., and Marc, R.E. (2016). Retinal remodeling in human retinitis pigmentosa. Exp. Eye Res. *150*, 149–165.

26. Gradinaru, V., Zhang, F., Ramakrishnan, C., Mattis, J., Prakash, R., Diester, I., Goshen, I., Thompson, K.R., and Deisseroth, K. (2010). Molecular and cellular approaches for diversifying and extending optogenetics. Cell *141*, 154–165.

27. Prusky, G.T., Alam, N.M., Beekman, S., and Douglas, R.M. (2004). Rapid quantification of adult and developing mouse spatial vision using a virtual optomotor system. Invest. Ophthalmol. Vis. Sci. *45*, 4611–4616.

28. van Wyk, M., Schneider, S., and Kleinlogel, S. (2015). Variable phenotypic expressivity in inbred retinal degeneration mouse lines: a comparative study of C3H/HeOu and FVB/N rd1 mice. Mol. Vis. *21*, 811–827.

29. Macé, E., Caplette, R., Marre, O., Sengupta, A., Chaffiol, A., Barbe, P., Desrosiers, M., Bamberg, E., Sahel, J.A., Picaud, S., et al. (2015). Targeting channelrhodopsin-2 to ON-bipolar cells with vitreally administered AAV restores ON and OFF visual responses in blind mice. Mol. Ther. *23*, 7–16.

30. Schiller, P.H., Sandell, J.H., and Maunsell, J.H. (1986). Functions of the ON and OFF channels of the visual system. Nature *322*, 824–825.

31. Sack, B.K., and Herzog, R.W. (2009). Evading the immune response upon in vivo gene therapy with viral vectors. Curr. Opin. Mol. Ther. *11*, 493–503.

32. Nagel, G., Szellas, T., Huhn, W., Kateriya, S., Adeishvili, N., Berthold, P., Ollig, D., Hegemann, P., and Bamberg, E. (2003). Channelrhodopsin-2, a directly light-gated cation-selective membrane channel. Proc. Natl. Acad. Sci. USA *100*, 13940–13945.

33. Klapoetke, N.C., Murata, Y., Kim, S.S., Pulver, S.R., Birdsey-Benson, A., Cho, Y.K., Morimoto, T.K., Chuong, A.S., Carpenter, E.J., Tian, Z., et al. (2014). Independent optical excitation of distinct neural populations. Nat. Methods *11*, 338–346.

34. Perny, M., Muri, L., Dawson, H., and Kleinlogel, S. (2016). Chronic activation of the D156A point mutant of channelrhodopsin-2 signals apoptotic cell death: the good and the bad. Cell Death Dis. *7*, e2447.

35. Berry, M.H., Holt, A., Salari, A., Veit, J., Visel, M., Levitz, J., Aghi, K., Gaub, B.M., Sivyer, B., Flannery, J.G., and Isacoff, E.Y. (2019). Restoration of high-sensitivity and adapting vision with a cone opsin. Nat. Commun. *10*, 1221.

36. Gill, J.S., Georgiou, M., Kalitzeos, A., Moore, A.T., and Michaelides, M. (2019). Progressive cone and cone-rod dystrophies: clinical features, molecular genetics and prospects for therapy. Br. J. Ophthalmol. *103*, 711.

37. Campochiaro, P.A., and Mir, T.A. (2018). The mechanism of cone cell death in retinitis pigmentosa. Prog. Retin. Eye Res. *62*, 24–37.

38. Boye, S.E., Alexander, J.J., Witherspoon, C.D., Boye, S.L., Peterson, J.J., Clark, M.E., Sandefer, K.J., Girkin, C.A., Hauswirth, W.W., and Gamlin, P.D. (2016). Highly efficient delivery of adeno-associated viral vectors to the primate retina. Hum. Gene Ther. *27*, 580–597.

39. Yin, L., Greenberg, K., Hunter, J.J., Dalkara, D., Kolstad, K.D., Masella, B.D., Wolfe, R., Visel, M., Stone, D., Libby, R.T., et al. (2011). Intravitreal injection of AAV2 transduces macaque inner retina. Invest. Ophthalmol. Vis. Sci. *52*, 2775–2783.

40. Dalkara, D., Kolstad, K.D., Caporale, N., Visel, M., Klimczak, R.R., Schaffer, D.V., and Flannery, J.G. (2009). Inner limiting membrane barriers to AAV-mediated retinal transduction from the vitreous. Mol. Ther. *17*, 2096–2102.

41. Cadigan, K.M., and Waterman, M.L. (2012). TCF/LEFs and Wnt signaling in the nucleus. Cold Spring Harb. Perspect. Biol. *4*, a007906.

42. Carroll, P.A., Freie, B.W., Mathsyaraja, H., and Eisenman, R.N. (2018). The MYC transcription factor network: balancing metabolism, proliferation and oncogenesis. Front. Med. *12*, 412–425.

43. Zeineddine, D., Hammoud, A.A., Mortada, M., and Boeuf, H. (2014). The Oct4 protein: more than a magic stemness marker. Am. J. Stem Cells *3*, 74–82.

44. Kim, S., Yu, N.-K., and Kaang, B.-K. (2015). CTCF as a multifunctional protein in genome regulation and gene expression. Exp. Mol. Med. *47*, e166.

45. Ikeda, K., Watanabe, Y., Ohto, H., and Kawakami, K. (2002). Molecular interaction and synergistic activation of a promoter by Six, Eya, and Dach proteins mediated through CREB binding protein. Mol. Cell. Biol. *22*, 6759–6766.

46. Li, X., Oghi, K.A., Zhang, J., Krones, A., Bush, K.T., Glass, C.K., Nigam, S.K., Aggarwal, A.K., Maas, R., Rose, D.W., and Rosenfeld, M.G. (2003). Eya protein phosphatase activity regulates Six1-Dach-Eya transcriptional effects in mammalian organogenesis. Nature *426*, 247–254.

47. Hsu, T., Trojanowska, M., and Watson, D.K. (2004). Ets proteins in biological control and cancer. J. Cell. Biochem. *91*, 896–903.

48. Kruse, E.A., Loughran, S.J., Baldwin, T.M., Josefsson, E.C., Ellis, S., Watson, D.K., Nurden, P., Metcalf, D., Hilton, D.J., Alexander, W.S., and Kile, B.T. (2009). Dual requirement for the ETS transcription factors Fli-1 and Erg in hematopoietic stem cells and the megakaryocyte lineage. Proc. Natl. Acad. Sci. USA *106*, 13814–13819.

49. Nagai, N., Ohguchi, H., Nakaki, R., Matsumura, Y., Kanki, Y., Sakai, J., Aburatani, H., and Minami, T. (2018). Downregulation of ERG and FLI1 expression in endothelial cells triggers endothelial-to-mesenchymal transition. PLoS Genet. *14*, e1007826.

50. Kent, W.J., Sugnet, C.W., Furey, T.S., Roskin, K.M., Pringle, T.H., Zahler, A.M., and Haussler, D. (2002). The human genome browser at UCSC. Genome Res. *12*, 996–1006.

51. Kuhn, R.M., Haussler, D., and Kent, W.J. (2013). The UCSC genome browser and associated tools. Brief. Bioinform. *14*, 144–161.

52. Altschul, S.F., Gish, W., Miller, W., Myers, E.W., and Lipman, D.J. (1990). Basic local alignment search tool. J. Mol. Biol. *215*, 403–410.

53. NCBI Resource Coordinators (2018). Database resources of the National Center for Biotechnology Information. Nucleic Acids Res. *46* (D1), D8–D13.

54. Jeon, C.J., Strettoi, E., and Masland, R.H. (1998). The major cell populations of the mouse retina. J. Neurosci. *18*, 8936–8946.

55. Wässle, H., Puller, C., Müller, F., and Haverkamp, S. (2009). Cone contacts, mosaics, and territories of bipolar cells in the mouse retina. J. Neurosci. *29*, 106–117.

56. Odermatt, P., Trüb, J., Furrer, L., Fricker, R., Marti, A., and Schümperli, D. (2016). Somatic therapy of a mouse SMA model with a U7 snRNA gene correcting SMN2 splicing. Mol. Ther. *24*, 1797–1805.

57. McFarland, T.J., Zhang, Y., Atchaneeyaskul, L.O., Francis, P., Stout, J.T., and Appukuttan, B. (2006). Evaluation of a novel short polyadenylation signal as an alternative to the SV40 polyadenylation signal. Plasmid *56*, 62–67.

58. Romijn, H.J. (1988). Development and advantages of serum-free, chemically defined nutrient media for culturing of nerve tissue. Biol. Cell *63*, 263–268.

59. R Development Core Team (2019). R: A language and environment for statistical computing (R Foundation for Statistical Computing).